

Journal of Visualized Experiments

Patient-derived Tumor Explants as a “Live” Preclinical Platform for Predicting Drug Resistance in Patients

--Manuscript Draft--

Article Type:	Methods Article - JoVE Produced Video
Manuscript Number:	JoVE62130R1
Full Title:	Patient-derived Tumor Explants as a “Live” Preclinical Platform for Predicting Drug Resistance in Patients
Corresponding Author:	Giuditta Viticchié, Ph.D. University of Leicester College of Life Sciences Leicester, Leicestershire UNITED KINGDOM
Corresponding Author's Institution:	University of Leicester College of Life Sciences
Corresponding Author E-Mail:	gv51@leicester.ac.uk
Order of Authors:	Giuditta Viticchié Ian Powley Constantinos Demetriou James Cooper Michael Butterworth Meeta Patel Naila Abid Gareth Miles Lynne Howells Howard Pringle Marion MacFarlane Catrin Pritchard
Additional Information:	
Question	Response
Please specify the section of the submitted manuscript.	Cancer Research
Please indicate whether this article will be Standard Access or Open Access.	Standard Access (US\$2,400)
Please indicate the city, state/province, and country where this article will be filmed . Please do not use abbreviations.	Nottingham, United Kingdom
Please confirm that you have read and agree to the terms and conditions of the author license agreement that applies below:	I agree to the UK Author License Agreement (for UK authors only)
Please provide any comments to the journal here.	

TITLE:

Patient-derived Tumor Explants as a “Live” Preclinical Platform for Predicting Drug Resistance in Patients

AUTHORS AND AFFILIATIONS:

Giuditta Viticchié¹, Ian Powley¹, Constantinos Demetriou¹, James Cooper¹, Michael Butterworth¹, Meeta Patel¹, Naila Abid¹, Gareth Miles¹, Lynne Howells¹, Howard Pringle¹, Marion MacFarlane², Catrin Pritchard¹

¹Leicester Cancer Research Center, University of Leicester, UK

²MRC Toxicology Unit, Hodgkin Building, Lancaster Road, Leicester, UK

Email addresses of co-authors:

Ian Powley	(irp2@le.ac.uk)
Constantinos Demetriou	(cd317@le.ac.uk)
James Cooper	(jc768@le.ac.uk)
Michael Butterworth	(mb777@le.ac.uk)
Meeta Patel	(mp598@le.ac.uk)
Naila Abid	(na328@le.ac.uk)
Gareth Miles	(gim14@le.ac.uk)
Lynne Howells	(lh28@le.ac.uk)
Howard Pringle	(jhp@le.ac.uk)
Marion MacFarlane	(mm21@le.ac.uk)
Catrin Pritchard	(cap8@le.ac.uk)

Corresponding author:

Giuditta Viticchié [\(gv51@le.ac.uk\)](mailto:gv51@le.ac.uk)

KEYWORDS:

explants, tumor, preclinical models, histology, digital pathology, multi-immunofluorescence

SUMMARY:

This paper describes methods for the generation, drug treatment, and analysis of patient-derived explants for assessing tumor drug responses in a live, patient-relevant, preclinical model system.

ABSTRACT:

An understanding of drug resistance and the development of novel strategies to sensitize highly resistant cancers rely on the availability of suitable preclinical models that can accurately predict patient responses. One of the disadvantages of existing preclinical models is the inability to contextually preserve the human tumor microenvironment (TME) and accurately represent intratumoral heterogeneity, thus limiting the clinical translation of data. By contrast, by representing the culture of live fragments of human tumors, the patient-derived explant (PDE) platform allows drug responses to be examined in a three-dimensional (3D) context that mirrors the pathological and architectural features of the original tumors as closely as possible. Previous

reports with PDEs have documented the ability of the platform to distinguish chemosensitive from chemoresistant tumors, and it has been shown that this segregation is predictive of patient responses to the same chemotherapies. Simultaneously, PDEs allow the opportunity to interrogate molecular, genetic, and histological features of tumors that predict drug responses, thereby identifying biomarkers for patient stratification as well as novel interventional approaches to sensitize resistant tumors. This paper reports PDE methodology in detail, from collection of patient samples through to endpoint analysis. It provides a detailed description of explant derivation and culture methods, highlighting bespoke conditions for particular tumors, where appropriate. For endpoint analysis, there is a focus on multiplexed immunofluorescence and multispectral imaging for the spatial profiling of key biomarkers within both tumoral and stromal regions. By combining these methods, it is possible to generate quantitative and qualitative drug response data that can be related to various clinicopathological parameters and thus potentially be used for biomarker identification.

INTRODUCTION:

The development of effective and safe anticancer agents requires appropriate preclinical models that can also provide insight into mechanisms of action that can facilitate the identification of predictive and pharmacodynamic biomarkers. Inter- and intratumor heterogeneity¹⁻⁵ and the TME⁶⁻¹² are known to influence anticancer drug responses, and many existing preclinical cancer models such as cell lines, organoids, and mouse models are not able to fully accommodate these crucial features. An “ideal” model is one that can recapitulate the complex spatial interactions of malignant with non-malignant cells within tumors as well as reflect the regional differences within tumors. This article focuses on PDEs as an emerging platform that can fulfil many of these requirements¹³.

The first example of the use of human PDEs, also known as histocultures, dates back to the late 1980s when Hoffman et al. generated slices of freshly resected human tumors and cultured them in a collagen matrix^{14,15}. This involved establishing a 3D culture system that preserved tissue architecture, ensuring the maintenance of stromal components and cell interactions within the TME. Without deconstructing the original tumor, Hoffman et al.¹⁶ heralded a new approach of translational research, and since this time, many groups have optimized different explant methods with the aim of preserving the tissue integrity and generating accurate drug response data¹⁷⁻²⁴, although some differences between protocols are evident. Butler et al. cultured explants in gelatin sponges to help the diffusion of nutrients and drugs through the specimen^{20,21,25}, whereas Majumder et al. created a tumor ecosystem by culturing explants on top of a matrix composed of tumor and stromal proteins in the presence of autologous serum derived from the same patient^{22,23}.

More recently, this group set up a protocol whereby explants are generated by fragmentation of tumors into 2–3 mm³-sized pieces that are then placed without additional components on permeable membranes at the air-liquid interface of a culture system²⁴. Taken together, these numerous studies have demonstrated that PDEs allow the culture of intact, live fragments of human tumors that retain the spatial architecture and regional heterogeneity of the original tumors. In original experiments, explants or histocultures were usually subjected to

homogenization following drug treatment, after which various viability assays were applied to the homogenized samples such as the histoculture drug response assay^{20,21}, the MTT (3-(4,5-dimethylthiazol-2-yl)-2,5-diphenyltetrazolium bromide) assay, the lactate dehydrogenase assay, or the resazurin-based assay²⁶⁻²⁸. Recent progress in endpoint analysis techniques, particularly digital pathology, have now expanded the repertoire of endpoint tests and assays that can be performed on explants^{29,30}. To apply these new technologies, instead of homogenization, explants are fixed in formalin, embedded in paraffin (FFPE) and then analyzed using immunostaining techniques, allowing spatial profiling. Examples of this approach have been documented for non-small cell lung cancer (NSCLC), breast cancer, colorectal cancer, and mesothelioma explants whereby immunohistochemical staining for the proliferation marker, Ki67, and the apoptotic marker, cleaved poly-ADP ribose polymerase (cPARP), was used to monitor changes in cell proliferation and cell death^{24,31-34}.

Multiplexed immunofluorescence is particularly amenable for spatial profiling of drug responses in explants at endpoint³⁵. For example, it is possible to measure the relocalization and spatial distribution of specific classes of immune cells, such as macrophages or T cells, within the TME upon drug treatment^{13,36-38}, and investigate whether a therapeutic agent can favor the transition from “cold tumor” to “hot tumor”³⁹. In recent years, this group has focused on the derivation of PDEs from different tumor types (NSCLC, renal cancer, breast cancer, colorectal cancer, melanoma) and the testing of a range of anticancer agents including chemotherapies, small-molecule inhibitors, and immune checkpoint inhibitors (ICIs). Endpoint analysis methods have been optimized to include multiplexed immunofluorescence to allow spatial profiling of biomarkers for viability as well as biomarkers for different constituents of the TME.

PROTOCOL:

NOTE: Tissue collection and processing of human cancer specimens were performed in compliance with the NHS Confidentiality Code of Practice and with the Data Protection Act 1998 of the University Hospitals of Leicester NHS Trust policy and procedure. A summary of the protocol steps is shown in **Figure 1**. Details of reagents and equipment are provided in the **Table of Materials**.

1. Tissue collection

1.1. After surgery, transfer freshly resected human tumor specimens into a tube containing 25 mL of fresh culture medium (Dulbecco's modified Eagle medium (supplemented with 4.5 g/L glucose and L-glutamine) + 1% (v/v) fetal calf serum + 1% penicillin–streptomycin) and stored on ice. Process the explant within 2 h of surgery in a sterile class II hood.

2. Explant preparation

2.1. Clean all surgical equipment (graft blades/dental wax surface/tweezers) with 70% industrial methylated spirit (IMS) solution.

2.2. Fill a 10 cm culture dish (see the **Table of Materials**) with ~25 mL of fresh medium, and place it on top of a bed of ice.

2.3. Using tweezers, transfer the specimen onto a dental wax surface (see the **Table of Materials**), and slice the tissue into fragments of approximately 2–3 mm³ using two skin graft blades.

NOTE: For best performance, start slicing the tissue to obtain an individual strip of 2–3 mm of thickness, and then cut the strip along the length to obtain the final explants. Repeat the process until the whole specimen is chopped.

2.4. Transfer the explants promptly into the ice-cold culture medium in the 10 cm dish. Take a proportion of the explants (6–9 pieces), place them in a 1 mL tube containing 10% of non-buffered formalin solution, and leave at room temperature (RT) for 24 h.

NOTE: These fragments will represent the control explants for the “uncultured” condition.

2.5. Fill the desired number of wells of 6-well plates with 1.5 mL of fresh medium per well, and place an organotypic culture insert disc (see the **Table of Materials**) in each well so that it floats on top of the medium, carefully avoiding air bubbles at the media-insert interface.

2.6. Select explants randomly, and place them one at a time on top of the insert disc. To be consistent with the “uncultured” condition, use 6–9 explants per well. Place the multiwell plate in a CO₂ incubator at 37 °C and 5% CO₂, and allow the explants to recover for 16 h.

NOTE: To avoid crushing the tissue, gentle handling of the tweezers is highly recommended.

3. Drug treatment

3.1. After 16 h, take new 6-well plates, add 1.5 mL of fresh medium to each well, add the relevant drugs at the desired concentrations, and include a well for the vehicle control. Using the tweezers, move each insert containing the explants to the newly prepared 6-well plates containing the drugs. Place the plates in the CO₂ incubator at 37 °C and 5% CO₂ for 24–48 h.

3.2. Transfer the uncultured explants previously fixed in formalin into a histology cassette (see section 4 below), and store in 70% IMS until the end of the experiment.

4. Histological processing

4.1. Tissue fixation

4.1.1. After drug treatment, transfer the insert discs containing the explants into new 6-well plates containing 10% formalin, and add a few drops of 10% formalin onto the top of the explants to ensure complete coverage with the fixative.

CAUTION: Formalin is hazardous. Avoid any contact with skin, and handle it inside a fume hood to prevent inhalation.

4.1.2. Allow the explants to remain overnight (20–24 h) in the 10% formalin.

4.1.3. On the next day, soak the relevant number of small histology sponges in 70% IMS, and place them inside histology cassettes. Gently transfer all the explants from a given drug treatment condition onto a single sponge (maintain the orientation of the explants so that the sides of the explants in contact with the insert discs, and therefore the drug-treated areas, are placed in contact with the sponge). Place another presoaked sponge on top of the explants, and secure within a histology cassette (one cassette per well/treatment).

4.1.4. Submerge the cassettes in 70% IMS, and leave at RT for 24 h.

4.2. Paraffin embedding and tissue sectioning

4.2.1. On the following day, transfer the histology cassettes containing the explants into the sample basket of the tissue processor (see the **Table of Materials**), and secure the lid. Place the basket in the retort and close gently. Select the desired program, and start the processor. Drain the retort, open it to remove the basket, and transfer the basket into the embedding center wax bath.

4.2.2. After embedding, transfer the metal cassette lids into the basket, and return to the retort of the tissue processor for the cleaning program. Wipe the sensor with a dry tissue, remove any excess wax from the retort lid, and proceed with the cleaning program.

4.2.3. Position a paraffin block in the rotary microtome, cut a few sections at 4 μm , and return the block to ice. Reposition the block, and cut more 4 μm sections. Transfer the sections with a small paint brush and forceps onto a water bath to remove creases and bubbles.

4.2.4. Position the sections centrally onto microscope slides, drain the slides for few minutes, and place them into a slide rack to dry overnight in an incubator at 37 °C. When the sections are dry, store them at RT in a slide folder or box to protect from dust.

5. Hematoxylin and eosin (H&E) staining

5.1. Fill the stainer (see the **Table of Materials**) with reagents, and set the required program for H&E staining: hematoxylin incubation time: 5 min; eosin incubation time: 3 min.

5.2. Attach the slide rack to the carrier, place it into the first container with xylene, and start the program. Remove the slide carrier from the rack, and take the container with the slide rack to the mounting area.

5.3. Mount the slides with dibutyl phthalate xylene (DPX) under the extraction hood. Place DPX onto each coverslip, and lower the slide onto the coverslip with the section downwards, allowing the DPX to spread out.

NOTE: DPX is hazardous. Avoid any contact with skin and use in a designated fume hood.

6. Immunostaining

NOTE: The following steps should be carried out at RT unless stated otherwise.

6.1. Deparaffinization and rehydration

6.1.1. Place the slides in a slide rack, and heat at 65 °C for 10 min before deparaffinizing the sections in xylene for 3 min (2x). Minimize the amount of carry-over solution.

NOTE: Xylene is flammable, hazardous, and irritant. Handle inside the fume hood whilst using double-layered gloves. Avoid skin and eye contact. Dispose of waste within a sealed container.

6.1.2. Rehydrate the slides in an alcohol gradient as follows: 99% IMS for 1 min (2x) and 95% IMS for 1 min. Minimize the amount of carry-over solution.

NOTE: IMS is highly flammable, volatile, and irritant. Handle inside the fume hood, and avoid skin and eye contact.

6.1.3. Completely submerge the slide rack in ultrapure (UP) water for 5 min.

6.2. Antigen retrieval

6.2.1. Prepare antigen retrieval buffer according to the manufacturer's guidelines for the particular antibody used.

NOTE: Citrate buffer 0.2 M, pH 6, or tris(hydroxymethyl)aminomethane (Tris)-ethylenediamine tetraacetic acid (EDTA) 0.1 M, pH 9, are the common buffers used for acidic or alkaline conditions, respectively. Citric acid monohydrate and Tris are irritant agents. Prepare all stock solutions in the fume hood. Avoid contact with skin and eyes.

6.2.2. Submerge the rack containing the slides into antigen retrieval buffer, and microwave (see the **Table of Materials**) at full power (800 W) for 20 min.

NOTE: Keep the slides fully submerged in the buffer during the entire process. To avoid excessive reduction of the buffer volume, place a lid on top of the container used.

6.3. Multiplex immunofluorescence (mIF)

NOTE: This process takes 1–2 days.

6.3.1. Fill a clean container with 250 mL of UP water, and completely submerge the slide rack for 2 min (2x). Proceed with assembling each slide into a slide coverplate (see the **Table of Materials**).

6.3.1.1. To assemble a slide onto a coverplate, prepare a glass trough with water. Submerge both the coverplate and slide in the water, placing the tissue section side facing the coverplate.

6.3.1.2. Position the bottom edge of the slide on top of the protuberances at the bottom of the coverplate, and finally align the slide to the coverplate, allowing the water to fill the gap in between with no air trapped. Hold the coverplate and slide together, and place them in a coverplate rack.

6.3.2. Fill the coverplate with phosphate-buffered saline (PBS), and wait for the buffer to wash the slides, flowing out by gravity (2x). Pipet 110 μ L of blocking buffer (see the **Table of Materials**) onto each coverplate and incubate for 10 min.

6.3.3. Prepare the desired primary antibody dilution in PBS or blocking buffer according to the manufacturer's recommendations. Incubate the slides with primary antibody (110 μ L each slide) for 30 min. Wash the slides with 5 mL of PBS (2x), as described in 6.3.2.

6.3.4. Incubate the slides with 110 μ L of horseradish peroxidase polymer for 30 min. Wash the slides with 5 mL of PBS (2x), as described in 6.3.2.

6.3.5. Prepare fluorophore dilution in amplification diluent 1:100 (v/v), and incubate the slides with fluorophore (110 μ L each slide) for 10 min. Wash the slides with 5 mL of PBS (2x), as described in 6.3.2.

NOTE: For the use of fluorophore 780, follow the manufacturer's guidelines. The experiment may be paused here if the slides are incubated in the final wash of PBS and stored at 4 °C overnight.

6.3.6. Unclip the slides from the coverplates, and go back to the antigen retrieval step to start the staining with a different antibody. Repeat the staining for the desired number of antibodies to be tested.

6.3.7. Following step 6.3.5 for the last fluorophore in use, keep the slides on the coverplates, prepare 6 μ M solution of 4'-6-diamidino-2-phenylindole (DAPI) dilactate with UP water, and counterstain the slides for 5 min (110 μ L each slide). Wash the slides with UP water (2x), and remove excess water by drying the edges of the slides. Assemble the coverslips on the slides using mounting medium, and store at RT in the dark.

7. Scanning

NOTE: Slide scanning was performed using a multispectral automated imaging system (see the **Table of Materials**).

7.1. Assemble the slides into the carrier, and load them into the scanner in the desired order.

NOTE: It is recommended that a control slide be included in which no fluorophore or DAPI is used during immunohistochemical staining. This slide will be used as the control for intrinsic fluorescence (autofluorescence (AF)) of the tissue.

7.2. After launching the slide scanner software, select **Edit Protocol** from the **Home** page. Create a new protocol addressing the **name**, **imaging mode**, the **type of multispectral scan** to be performed (**4–7 channels**), and study (**directory**).

NOTE: To modify the default settings of bands analyzed, select/deselect the desired filters using the function **Select Scan Bands**.

7.3. Proceed with **Scan Exposure** and **Load carrier**, and finally select the **carrier** for the protocol setup. Select **Take Overview** to detect the tissue on the slide. Choose a **slide** displayed on the **carrier**, and select a **specific area of the tissue** with the red cursor to bring it into live view on the left window of the screen.

7.4. Select the **DAPI filter**, and click on **Autofocus** or manually adjust the **Stage Height slider** to focus the field of interest. Click on **Autoexpose** to allow the system to find the best exposure for that filter/band.

NOTE: The exposure time for each filter is set at 12 ms. After autoexposing the system, refine the exposure time to a better estimate. It is also possible to override the autoexposure value by typing a value manually into the highlighted cell.

7.5. Repeat the above steps for all filters in the protocol. If necessary, change the locations and/or slides to find the best signals for setting the exposures.

NOTE: If the tissue is highlighted in red in live view, the fluorescent signal of the filter analyzed is saturated, and autoexposure must be repeated.

7.6. Once the exposure settings have been established, click on the **Back** button, and **Save** the protocol. From the software home page (see the **Table of Materials**), select **Scan Slides**.

7.7. Stack all the carriers to be scanned into the **Slide Carrier Hotel**, and take note of the order of the slides to assign their ID into the system.

NOTE: On the software screen, each carrier will be related to a slot containing 4 slides.

7.8. To configure multiple slides with the same parameters, click on **Configure Tasks**, and select one or more Slots with the option **Using the same rules for the same slides**. Once the **Edit Slides** opens, configure: **Tasks**, **Study**, and **Protocol**, and click on **OK**.

7.9. Label each slide by clicking on the **Slot** icon, and type a name in the **Slide ID** cell. Click on **Scan** to start scanning.

NOTE: Once the **Slot** icon turns blue and the slides are marked with a blue arrow, the carrier has all the rules and is ready to be scanned. It is possible to save the slide IDs, studies, protocols, and tasks by clicking on the **Save Setup** button.

8. Analysis

NOTE: The protocol below illustrates the method for phenotype analysis.

8.1. Image preparation

8.1.1. To prepare the images for analysis, open the viewer software (see the **Table of Materials**), and select **Load slides**. Select the desired scans for the training project on the right-hand side of the screen.

8.1.2. For each scan, click on **Stamp**, and choose **Project** in the box **Select for:**. Define a stamp with size 1 x 1 in the image field to be used later as a template for the training analysis. Observe that this stamp will be marked as a red square.

NOTE: The number of stamp annotations for the Project is arbitrary. It is recommended to generate one for the intrinsic fluorescence scan and a few more that are generally representative of the signal distribution within the tissue.

8.1.3. Finally, open all the scans of the experiment. For each one, click on **Stamp**, and this time, choose **the option Batch** in the box **Select for:**. Place a stamp circumscribing each explant.

NOTE: This time, the stamps will be marked as green squares and will be required once the batch analysis is launched. Choose the appropriate size for the stamps (1 x 1, 2 x 2, 3 x 3) and avoid overlapping of the stamps, which would generate duplicated data in the exported file.

8.2. Training analysis

8.3. Launch the software for analysis (see the **Table of Materials**), and create a new project: **Select File | New | Project**.

8.4. Type a name in the **Project Name** box, and configure the **type of project**.

NOTE: The experiments were performed using the following specifications: trainable tissue segmentation; adaptive cell segmentation; phenotyping.

8.5. Load the scans containing the stamps for training: **File | Open | Image**. In **single mode view**, navigate through the images and select the scans with intrinsic fluorescence.

8.6. Click on the **Autofluorescence (AF)** button, and with the **Autofluorescence picker**, draw on an unstained portion of tissue. Click on **Prepare images** to allow the software to subtract the intensity of intrinsic fluorescence from all the images uploaded for training.

8.7. Click on the **Edit Markers and Colors** button, and enter the **marker names** in the box associated with their fluorophore. Click on the **Segment Tissue** step on top of the screen to open the **Tissue Segmentation Training** window.

8.8. In the **Tissue Categories** window, type in the **name of the tissue categories** to segment the images into (e.g., **Tumor, Stroma, Background, Necrosis**).

8.9. In the **Tissue Segmentation Training** window, click on the **Draw** button and draw regions around groups of cells to define a tissue category of interest. For example, to define a **Tumor** area, draw a region around a group of tumor cells. Switch to the next category and repeat the drawing process.

NOTE: It is recommended to draw regions in most of the images uploaded for training. It is also possible to refine the training by editing the **Pattern Scale** and the **Segmentation Resolution** whose details are better described in the user manual.

8.10. Having defined the training regions, proceed with **Train the Tissue Segmenter**.

NOTE: During the process of training, the software displays the percentage of accuracy of tissue segmentation. For optimal results, it is recommended that tissue segmentation be at least 90% accurate. Once the Segmenter has stabilized, click on the **Done** button.

8.11. To see the **Tissue Category** mask on all images, click on the **Segment All** button.

8.12. **After verifying the quality of tissue segmentation**, re-draw the training regions around the areas that were incorrectly classified, and re-train the **Tissue Segmenter** until the process is successful.

8.13. Click on the **Cell Segmentation** step in the **Step Bar** at the top of the window to proceed with the analysis.

8.14. Choose the cellular compartments to segment: **Nuclei, Cytoplasm, and/or Membrane**.

NOTE: As adaptive cell segmentation can only detect cells with nuclear signal, do not de-select **Nuclei**. Although it is also possible to segment cytoplasm and/or membrane, it is recommended to choose the strongest, most abundant nuclear component first (e.g., DAPI).

8.15. Configure the nuclear component using the **Typical Intensity** slider to adjust the threshold used to detect nuclear pixels. Take note of the preview window that opens and provides live feedback as the threshold is adjusted.

NOTE: This threshold is adaptive and is measured relative to the surrounding background. Increase this value if too much background is detected as nuclear. Lower this value if faint nuclei are being missed. Use the **Show/Hide Regions** button to blink the segmentation masks on and off, and check whether the correct pixels are being detected as nuclear.

8.16. To split clusters of nuclear pixels, use the **Nuclear Component Splitting** panel. Choose the button that best describes the staining quality of the nuclei. Then, use the slider bar to adjust the **Splitting Sensitivity**, keeping in mind that lower values will result in more splitting.

8.17. Click on the **Segment All** button to segment all the images. If the result is not accurate, modify the settings and re-train the software until a satisfying segmentation is achieved.

8.18. Proceed to the last step of the analysis: **Phenotyping**. In the **Phenotypes** panel, add the list of phenotypes to be detected, and type the **name** in the corresponding text box. Click on the **Edit Phenotypes** button, select a particular cell to bring up a dropdown menu, and choose the corresponding phenotype.

NOTE: At least five cells for each phenotype are necessary to train the classifier. Turning off the visualization of the nuclei allows better visualization of the cell phenotype that needs to be assigned.

8.19. Once the selection for training is complete, click on the **Train Classifier** button.

NOTE: The software will classify every single cell in the image, and whenever errors in classification occur, it is possible to edit the phenotype of the cells and repeat the training of the classifier. Save the project before proceeding to batch analysis, and click on the **Export** function in the tool bar on the top of the screen.

8.20. Select the **Bath Analysis** tab on the left menu, and load the project in the **Batch Algorithm** or **Project** box.

8.21. Click on **Export Options** to create separate directories for each image, and with the **Browse** button, navigate to find the location to export the data. Click on all the options of the **Images** and **Tables** to export.

8.22. On the right side of the screen, click on **Add Slides** and load all the images containing stamps for previously prepared batches (step 7.3). Click on the **Run** button to start the batch analysis and process one stamp at a time, exporting the corresponding data.

REPRESENTATIVE RESULTS:

Multispectral imaging of mIF-stained histological sections permits identification and phenotyping of individual cell populations and identification of tumor and stromal components in the explant TME (**Figure 2**). Multispectral imaging is particularly useful for the analysis of tissues with high intrinsic autofluorescence, such as tissue with a high collagen content, as it allows the autofluorescence signal to be deconvoluted from other signals and excluded from subsequent analysis. Subsequent in silico tissue and cell segmentation allows the quantification of drug response with a multitude of outputs including, but not limited to, raw cell numbers (e.g., percent positivity), signal intensity, cell size, tissue area, and spatial location of individual cells.

Tissue and cell segmentation are therefore extremely useful for the quantitative analysis of drug treatment outcomes and the identification of tumor- and stromal-specific responses. For example, staining for Ki67 and cPARP alongside a tumor marker allows for the quantitation of proliferation and cell death levels, respectively, in explants (**Figure 3**). In the example given, Ki67 and cPARP levels are quantitated for stromal and tumor regions in PDEs in response to the anti-programmed cell death protein 1 (PD-1) immune checkpoint inhibitor (ICI), nivolumab. In addition, the ability to extract spatial information from stained sections allows the calculation of intercell distances as well as distances to tumor borders and other structures. Therefore, changes in cellular distribution following drug treatment can be quantitatively analyzed (**Figure 4**). The example shown represents PDE treatment with nivolumab.

FIGURE AND TABLE LEGENDS:

Figure 1: Workflow for the generation and analysis of PDEs. (A) Freshly resected human tumor specimens are processed and arranged on a permeable culture insert disc floating in culture medium. (B) Following drug treatment, the explants are harvested, subjected to FFPE, and then sectioned for histological analysis, e.g., for H&E staining. (C) mIF staining and scanning of the tissue sections are performed to generate multispectral images from which individual signals can be deconvoluted and analyzed separately. (D) Analysis of composite images allows separation of tumor and stromal areas and assessment of the phenotype of different cell types. Abbreviations: PDE = patient-derived explant; FFPE = fixed in formalin, embedded in paraffin; H&E = hematoxylin and eosin; mIF = multiplex immunofluorescence; HRP = horseradish peroxidase; H₂O₂ = hydrogen peroxide; Ab = antibody; TSA = tyramide signal amplification.

Figure 2: Example of an mIF-stained tissue section. NSCLC explant tissue was stained for markers of cell viability, namely, cPARP (red) and Ki67 (green) as well as a pan-cytokeratin marker (yellow) and DAPI (blue) to mark nuclei. Multispectral imaging was performed to deconvolute the fluorescent signals and remove autofluorescence. Images show 20x magnification of the selected field. Scale bars = 50 μ m. Abbreviations: mIF = multiplex immunofluorescence; NSCLC = non-small cell lung cancer; cPARP = cleaved poly-ADP ribose polymerase; CK = cytokeratin; DAPI = 4'-6-

diamidino-2-phenylindole; AF = autofluorescence.

Figure 3: Quantification of cell death and proliferation in PDEs. Example of box and whisker plots showing apoptosis induction in NSCLC PDEs after 24 h of treatment with 5 µg/mL nivolumab compared to medium control. The percentage of proliferation (Ki67) and percentage of apoptotic cell death (cPARP) events is displayed in the tumor area and stroma, respectively. Each point represents a single explant, the central line of the box represents the median of the distribution, and the sides of the box (bottom and top) represent the first and third quartiles, respectively. Error bars represent the interquartile range (further than 1.5 x IQR). Abbreviations: PDE = patient-derived explant; NSCLC = non-small cell lung cancer; cPARP = cleaved poly-ADP ribose polymerase; IQR = interquartile range.

Figure 4: Spatial organization following drug treatment. (A) Representative images showing mIF staining of T cell markers—CD4, FOXP3, CD8 (left panel)—performed on a melanoma explant, and corresponding phenotype analysis (right) identifying intercell distances between CD8+ cells and Treg cells (CD4+/FOXP3+). Scale bars = 200 µm. (B) Histogram plot showing increased distance between cytotoxic T cells (CD8+) and Treg cells (CD4+/FOXP3+) after treatment of melanoma PDEs with 5 µg/mL of nivolumab, confirming on-target effects of the IO drug. Density unit is expressed as the number of cells divided by sum of all cells per bandwidth. Abbreviations: mIF = multiplex immunofluorescence; CD = cluster of differentiation; FOXP3 = Forkhead box P3; PDE = patient-derived explant; NSCLC = non-small cell lung cancer; IO = immuno-oncology.

DISCUSSION:

This paper describes the methods for generation, drug treatment, and analysis of PDEs and highlights the advantages of the platform as a preclinical model system. Ex vivo culturing of a freshly resected tumor, which does not involve its deconstruction, allows for the retention of the tumor architecture^{13,24} and thus, the spatial interactions of cellular components in the TME as well as intratumoral heterogeneity. This method demonstrates how, by using a tumor-specific marker, it is possible to identify areas of tumor tissue versus areas of stroma and therefore separate drug responses within these compartments (**Figure 3**). Additionally, multiple biomarkers can be profiled simultaneously to assess, for example, the on-target movement of immune cells within the TME (**Figure 4**).

A previous publication documented the application of this PDE platform to the stratification of NSCLC PDEs for the standard of care chemotherapy, cisplatin, showing that it is possible to segregate chemoresistant from chemosensitive populations²⁴. These PDE-related findings mirror patient responses. By following the methods described here, it is possible to undertake similar approaches for other tumor types and with different types of drugs, chemotherapeutics or otherwise. The separation of PDEs into drug-sensitive and drug-resistant populations creates an invaluable resource for generating further mechanistic insight into drug resistance. For example, because PDEs can be processed for RNA, DNA, protein, or metabolite isolation, this can allow the implementation of “omic” technologies to identify key biomarkers that are predictive of response. Alternatively, FFPE sections generated from treated PDEs can be used for extensive spatial profiling to understand how different cell types in the PDE contribute to drug resistance.

This may be facilitated by further developments in multispectral imaging and mass cytometry approaches^{35,40–43}, which would allow hundreds of biomarkers to be profiled simultaneously. Preclinical models that evaluate immunotherapeutic efficacy are much sought after, and this paper demonstrates that PDEs can fill this critical niche (**Figure 3** and **Figure 4**). Monoclonal antibodies targeting immune checkpoints, such as cytotoxic T-lymphocyte antigen 4 and PD-1/programmed death ligand-1 (PD-L1), have been developed^{44–47} with some remarkable improvements in overall patient survival in a large number of solid tumors compared to standard chemotherapy. However, ICIs are effective in a limited number of patients for reasons that are not clear, necessitating the identification of predictive biomarkers⁴⁸. The outstanding feature of PDEs—preserving the 3D architecture of tumor tissue—facilitates the evaluation of ICI efficacy (**Figure 3**) and the monitoring of immune cells in response to ICI treatment (**Figure 4**). Thus, PDEs are an ideal platform for distinguishing ICI-sensitive versus ICI-resistant cases and for investigating the mechanisms underpinning this distinction.

PDE technology does suffer from a few disadvantages. The generation of accurate, experimental results from PDEs relies on tumor integrity, and occasionally, tumor samples after surgery are too necrotic to process for PDEs. Furthermore, despite some specific examples of retention of tissue integrity after prolonged culture²⁵, for most reported cases, integrity and viability has been lost after 72 h in culture, and tissue disintegration occurs. The window of time to perform drug experiments is therefore relatively limited, prohibiting the use of this model for the study of the mechanisms of acquired drug resistance or the study of invasion and metastasis¹³. Extending the viability of explants may become possible in the future through the development of new technologies, such as scaffolds and perfused channels, which may facilitate diffusion and uptake of nutrients, allowing more extended culture.

However, until these improvements can be made, the PDE platform should be regarded as a short-term culture method that can provide immediate drug response data. It should be utilized alongside other model systems, such as organoids and PDX models, that can provide longer term drug response data. Overall, the PDE platform is a proof-of-concept preclinical model system that is of use in determining the sensitivity of a patient's tumor to a given anticancer agent, for deriving insight into mechanisms of drug action in a real tumor, and for developing predictive and pharmacodynamic biomarkers.

ACKNOWLEDGMENTS:

We thank the surgeons and pathologists at University Hospitals of Leicester NHS Trust for providing surgical resected tumor tissue. We also thank the Histology facility within Core Biotechnology Services for help with tissue processing and sectioning of FFPE tissue blocks and Kees Straatman for support with use of the Vectra Polaris. This research was supported and funded by the Explant Consortium comprising four partners: The University of Leicester, The MRC Toxicology Unit, Cancer Research UK Therapeutic Discovery Laboratories, and LifeArc. Additional support was provided by the CRUK-NIHR Leicester Experimental Cancer Medicine Centre (C10604/A25151). Funding for GM, CD, and NA was provided by Breast Cancer Now's Catalyst Programme (2017NOVPCC1066), which is supported by funding from Pfizer.

DISCLOSURES:

Nothing to disclose

REFERENCES:

- 1 Gerlinger, M. et al. Intratumor heterogeneity and branched evolution revealed by multiregion sequencing. *The New England Journal of Medicine*. **366** (10), 883–892 (2012).
- 2 Jamal-Hanjani, M. et al. Tracking the evolution of non-small-cell lung cancer. *The New England Journal of Medicine*. **376** (22), 2109–2121 (2017).
- 3 McGranahan, N., Swanton, C. Biological and therapeutic impact of intratumor heterogeneity in cancer evolution. *Cancer Cell*. **27** (1), 15–26 (2015).
- 4 Casey, T. et al. Molecular signatures suggest a major role for stromal cells in development of invasive breast cancer. *Breast Cancer Research and Treatment*. **114** (1), 47–62 (2009).
- 5 Gerdes, M. J. et al. Emerging understanding of multiscale tumor heterogeneity. *Frontiers in Oncology*. **4**, 366 (2014).
- 6 Komohara, Y., Takeya, M. CAFs and TAMs: maestros of the tumour microenvironment. *The Journal of Pathology*. **241** (3), 313–315 (2017).
- 7 Miyake, M. et al. CXCL1-mediated interaction of cancer cells with tumor-associated macrophages and cancer-associated fibroblasts promotes tumor progression in human bladder cancer. *Neoplasia*. **18** (10), 636–646 (2016).
- 8 Hisamitsu, S. et al. Interaction between cancer cells and cancer-associated fibroblasts after cisplatin treatment promotes cancer cell regrowth. *Human Cell*. **32** (4), 453–464 (2019).
- 9 Witz, I. P. The tumor microenvironment: the making of a paradigm. *Cancer Microenvironment*. **2** (Suppl 1), 9–17 (2009).
- 10 Fu, X. T. et al. Tumor-associated macrophages modulate resistance to oxaliplatin via inducing autophagy in hepatocellular carcinoma. *Cancer Cell International*. **19**, 71 (2019).
- 11 Chen, D., Zhang, X. Tipping tumor microenvironment against drug resistance. *Journal of Oncology Translational Research*. **1** (1), 106 (2015).
- 12 Roma-Rodrigues, C., Mendes, R., Baptista, P. V., Fernandes, A. R. Targeting tumor microenvironment for cancer therapy. *International Journal of Molecular Sciences*. **20** (4), 840 (2019).
- 13 Powley, I. R. et al. Patient-derived explants (PDEs) as a powerful preclinical platform for anti-cancer drug and biomarker discovery. *British Journal of Cancer*. **122** (6), 735–744 (2020).
- 14 Freeman, A. E., Hoffman, R. M. In vivo-like growth of human tumors in vitro. *Proceedings of the National Academy of Sciences of United States of America*. **83** (8), 2694–2698 (1986).
- 15 Vescio, R. A. et al. In vivo-like drug responses of human tumors growing in three-dimensional gel-supported primary culture. *Proceedings of the National Academy of Sciences of United States of America*. **84** (14), 5029–5033 (1987).
- 16 Hoffman, R. M. 3D Sponge-matrix histoculture: an overview. *Methods in Molecular Biology*. **1760**, 11–17 (2018).
- 17 Vescio, R. A., Connors, K. M., Kubota, T., Hoffman, R. M. Correlation of histology and drug response of human tumors grown in native-state three-dimensional histoculture and in nude mice. *Proceedings of the National Academy of Sciences of United States of America*. **88** (12), 5163–5166 (1991).

- 18 Furukawa, T., Kubota, T., Hoffman, R. M. Clinical applications of the histoculture drug response assay. *Clinical Cancer Research*. **1** (3), 305–311 (1995).
- 19 Centenera, M. M., Raj, G. V., Knudsen, K. E., Tilley, W. D., Butler, L. M. Ex vivo culture of human prostate tissue and drug development. *Nature Reviews Urology*. **10** (8), 483–487 (2013).
- 20 Centenera, M. M. et al. Evidence for efficacy of new Hsp90 inhibitors revealed by ex vivo culture of human prostate tumors. *Clinical Cancer Research*. **18** (13), 3562–3570 (2012).
- 21 Dean, J. L. et al. Therapeutic response to CDK4/6 inhibition in breast cancer defined by ex vivo analyses of human tumors. *Cell Cycle*. **11** (14), 2756–2761 (2012).
- 22 Majumder, B. et al. Predicting clinical response to anticancer drugs using an ex vivo platform that captures tumour heterogeneity. *Nature Communications*. **6**, 6169 (2015).
- 23 Goldman, A. et al. Temporally sequenced anticancer drugs overcome adaptive resistance by targeting a vulnerable chemotherapy-induced phenotypic transition. *Nature Communications*. **6**, 6139 (2015).
- 24 Karekla, E. et al. Ex vivo explant cultures of non-small cell lung carcinoma enable evaluation of primary tumor responses to anticancer therapy. *Cancer Research*. **77** (8), 2029–2039 (2017).
- 25 Ricciardelli, C. et al. Novel ex vivo ovarian cancer tissue explant assay for prediction of chemosensitivity and response to novel therapeutics. *Cancer Letters*. **421**, 51–58 (2018).
- 26 Yoshimasu, T. et al. [Histoculture drug response assay (HDRA) guided induction concurrent chemoradiotherapy for mediastinal node-positive non-small cell lung cancer]. *Gan To Kagaku Ryoho. Cancer and chemotherapy*. **30** (2), 231–235 (2003).
- 27 Pirnia, F. et al. Ex vivo assessment of chemotherapy-induced apoptosis and associated molecular changes in patient tumor samples. *Anticancer Research*. **26** (3a), 1765–1772 (2006).
- 28 Maund, S. L., Nolley, R., Peehl, D. M. Optimization and comprehensive characterization of a faithful tissue culture model of the benign and malignant human prostate. *Laboratory Investigation*. **94** (2), 208–221 (2014).
- 29 Vasaturo, A., Galon, J. Multiplexed immunohistochemistry for immune cell phenotyping, quantification and spatial distribution in situ. *Methods in Enzymology*. **635**, 51–66 (2020).
- 30 Fuhrman, K. et al. Molecularly guided digital spatial profiling for multiplexed analysis of gene expression with spatial and single cell resolution. *Journal of Biomolecular Techniques*. **31** (Suppl), S14-15 (2020).
- 31 Twiddy, D. et al. A TRAIL-R1-specific ligand in combination with doxorubicin selectively targets primary breast tumour cells for apoptosis. *Breast Cancer Research*. **12** (1), P58 (2010).
- 32 Cai, H. et al. Cancer chemoprevention: Evidence of a nonlinear dose response for the protective effects of resveratrol in humans and mice. *Science Translational Medicine*. **7** (298), 298ra117 (2015).
- 33 Busacca, S. et al. Resistance to HSP90 inhibition involving loss of MCL1 addiction. *Oncogene*. **35** (12), 1483–1492 (2016).
- 34 Kolluri, K. K. et al. Loss of functional BAP1 augments sensitivity to TRAIL in cancer cells. *Elife*. **7**, e30224 (2018).
- 35 Toki, M. I. et al. High-plex predictive marker discovery for melanoma immunotherapy-treated patients using digital spatial profiling. *Clinical Cancer Research*. **25** (18), 5503–5512 (2019).

- 36 Parra, E. R. et al. Validation of multiplex immunofluorescence panels using multispectral microscopy for immune-profiling of formalin-fixed and paraffin-embedded human tumor tissues. *Scientific Reports*. **7** (1), 13380 (2017).
- 37 Park, I. J. et al. Prediction of radio-responsiveness with immune-profiling in patients with rectal cancer. *Oncotarget*. **8** (45), 79793–79802 (2017).
- 38 Mezheyski, A. et al. Multispectral imaging for quantitative and compartment-specific immune infiltrates reveals distinct immune profiles that classify lung cancer patients. *The Journal of Pathology*. **244** (4), 421–431 (2018).
- 39 Kather, J. N. et al. Topography of cancer-associated immune cells in human solid tumors. *Elife*. **7**, e36967 (2018).
- 40 Zollinger, D. R., Lingle, S. E., Sorg, K., Beechem, J. M., Merritt, C. R. GeoMx™ RNA assay: high multiplex, digital, spatial analysis of RNA in FFPE tissue. *Methods in Molecular Biology*. **2148** 331–345 (2020).
- 41 Zugazagoitia, J. et al. Biomarkers associated with beneficial PD-1 checkpoint blockade in non-small cell lung cancer (NSCLC) identified using high-plex digital spatial profiling. *Clinical Cancer Research*. **26** (16), 4360–4368 (2020).
- 42 Allo, B., Lou, X., Bouzekri, A., Ornatsky, O. Clickable and high-sensitivity metal-containing tags for mass cytometry. *Bioconjugate Chemistry*. **29** (6), 2028–2038 (2018).
- 43 Gerdtsson, E. et al. Multiplex protein detection on circulating tumor cells from liquid biopsies using imaging mass cytometry. *Convergent Science Physical Oncology*. **4** (1), 015002 (2018).
- 44 Reck, M. et al. Pembrolizumab versus chemotherapy for PD-L1-positive non-small-cell lung cancer. *The New England Journal of Medicine*. **375** (19), 1823–1833 (2016).
- 45 Le, D. T. et al. KEYNOTE-164: Phase 2 study of pembrolizumab for patients with previously treated, microsatellite instability-high advanced colorectal carcinoma. *Journal of Clinical Oncology*. **34** (15_suppl), TPS3631 (2016).
- 46 Diaz, L. A. et al. KEYNOTE-177: Randomized phase III study of pembrolizumab versus investigator-choice chemotherapy for mismatch repair-deficient or microsatellite instability-high metastatic colorectal carcinoma. *Journal of Clinical Oncology*. **35** (4_suppl), TPS815 (2017).
- 47 Long, G. V. et al. Impact of baseline serum lactate dehydrogenase concentration on the efficacy of pembrolizumab and ipilimumab in patients with advanced melanoma: data from KEYNOTE-006. *European Journal of Cancer*. **72**, S122–S123 (2017).
- 48 Voong, K. R., Feliciano, J., Becker, D., Levy, B. Beyond PD-L1 testing-emerging biomarkers for immunotherapy in non-small cell lung cancer. *Annals of Translational Medicine*. **5** (18), 376 (2017).

Figure 1

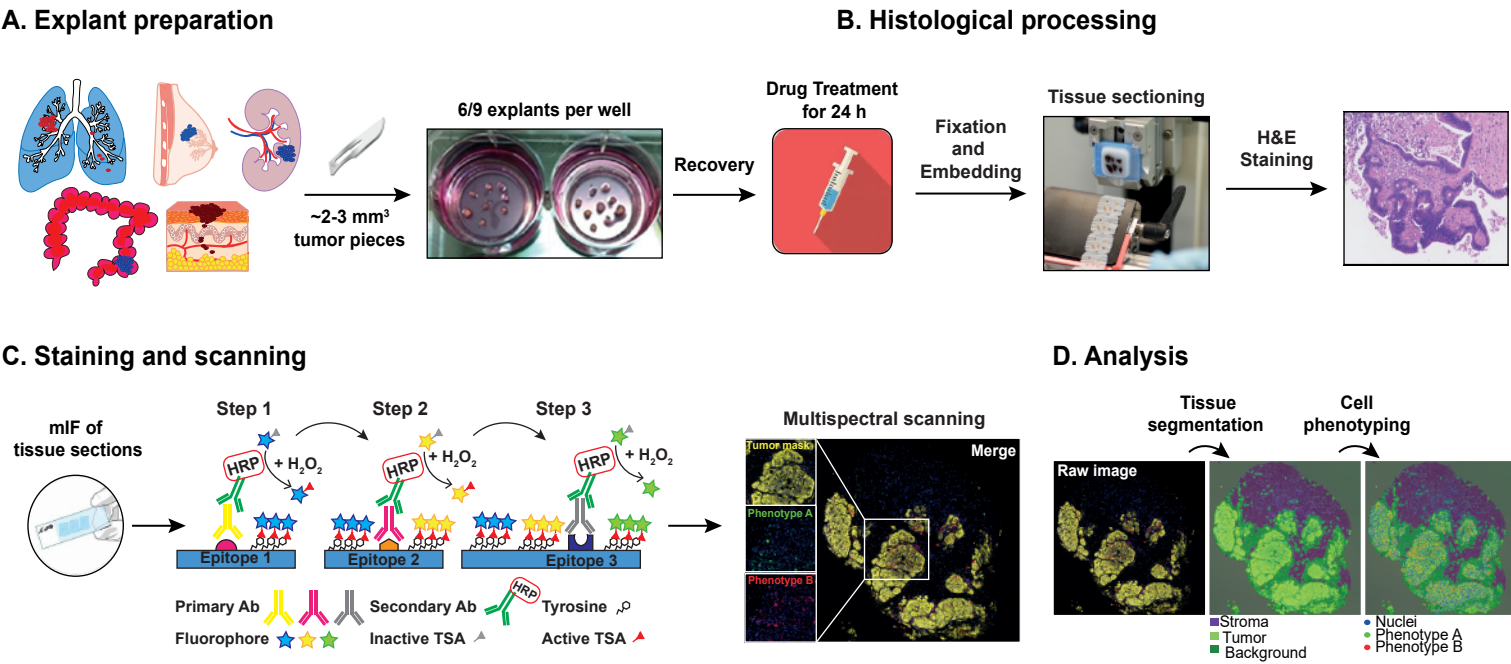


Figure 2

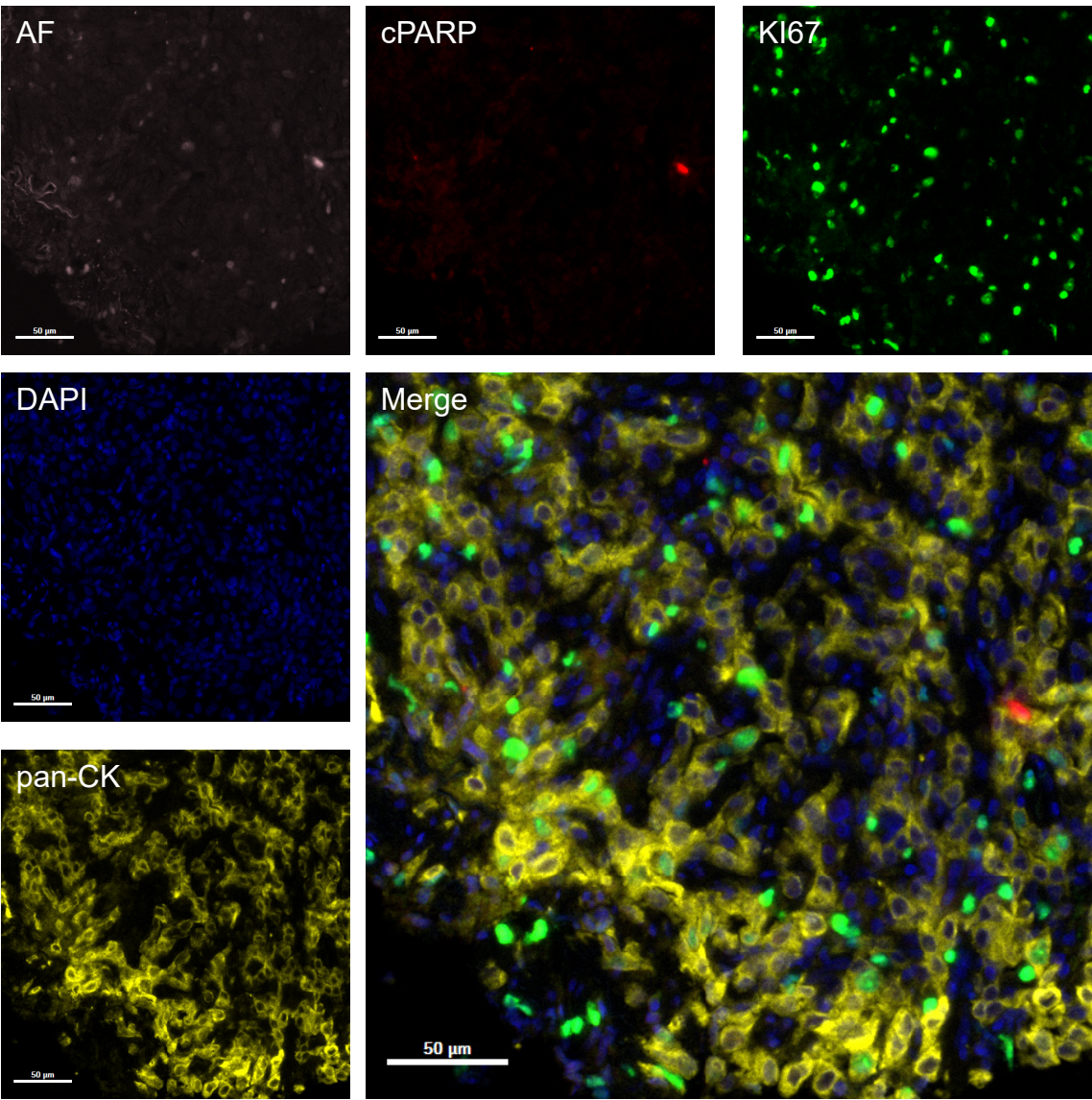


Figure 3

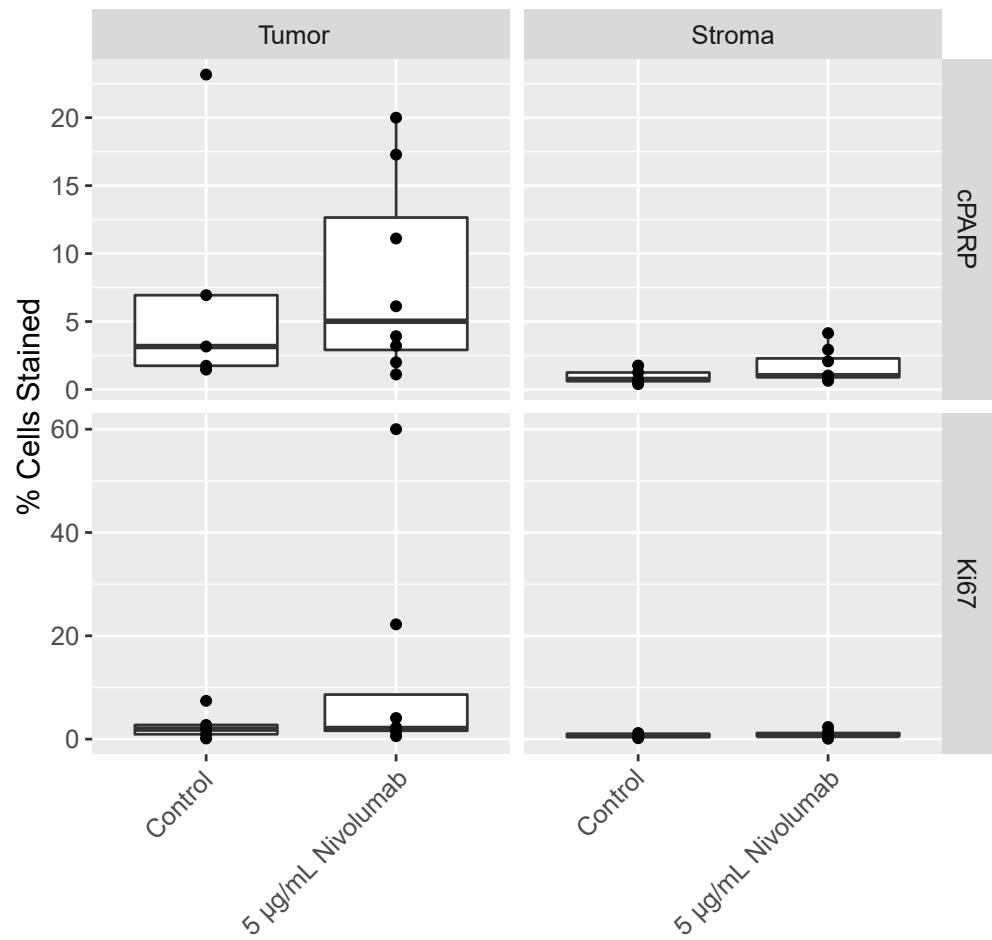
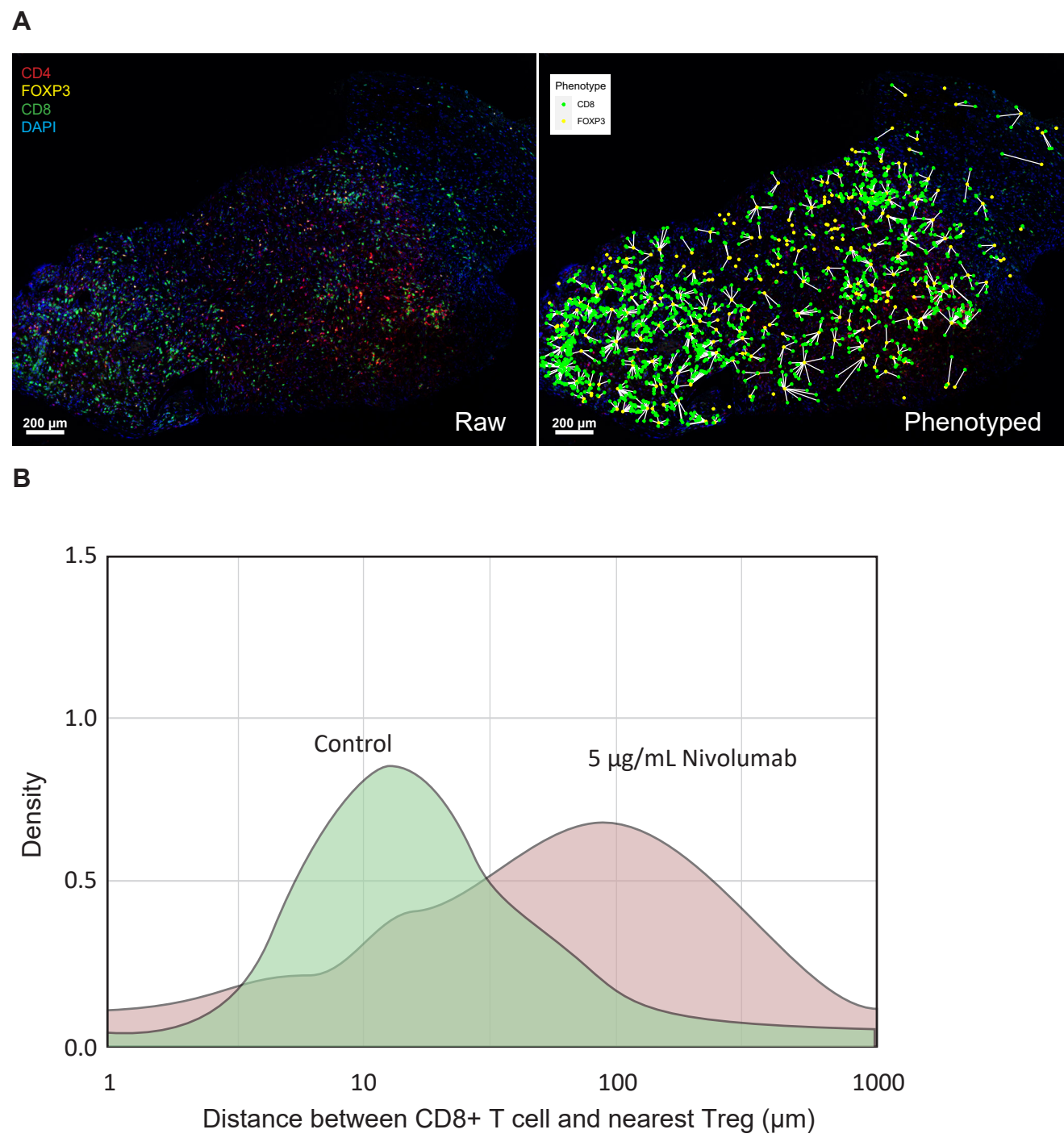


Figure 4



Name of Material/ Equipment
Acetic acid
Antibody Diluent / Block, 1x
Barnstead NANOpure Diamond
Citric Acid Monohydrate
Costar Multiple Well Cell Culture Plates
DAPI Dilactate
100 x 17 mm Dish, Nunclon Delta
DMEM (1x) Dubelcco's Modified Eagle Medium + 4.5 g/L D-Glucose + 110 mg/mL Sodium Pyruvate
DPX mountant
DPX mountant
Ethylenediaminetetraacetic acid (EDTA)
Eosin
Foetal Bovine Serum
37% Formaldehyde
iGenix, microwave oven IG2095
Industrial methylated spirit (IMS)
InForm Advanced Image Analysis Software
Leica ASP3000 Tissue Processor
Leica Arcadia H and C
Leica RM2125RT
Leica ST4040 Linear Stainer
Mayer's Haematoxylin
Millicell Cell Culture Inserts, 30 mm, hydrophilic PTFE, 0.4 µm
Novolink Polymer Detection System
OPAL 480
OPAL 520
OPAL 570
OPAL 620
OPAL 650
OPAL 690
OPAL 780 / OPAL TSA-DIG Reagent

Opal Polymer HRP Ms Plus Rb, 1x
Penicillin/streptomycin solution
PhenoChart Whole Slide Contextual Viewer
Phosphate Buffered Saline Tablets
1x Plus Amplification Diluent
Prolong Diamond Antifade Mountant
Slide Carrier
Sodium Chloride
Sodium Hydroxide pellets
Tenatex Toughened Wax - Pink (500 g)
Thermo Scientific Shandon Sequenza Slide Rack for Immunostaining Center
Thermo Scientific Shandon Plastic Coverplates
Tris(hydroxymethyl)aminomethane (Tris)
VectaShield
Vectra Polaris Slide Scanner
Xylene

Company	Catalog Number	Comments/Description
Sigma	320099	Staining reagent
Perkin Elmer	ARD1001EA	Antibody diluent/blocking buffer
Barnstead		Ultra Pure (UP) H ₂ O machine
Sigma-Aldrich	C7129	Reagent for citrate buffer
Corning Incorporated	3516	6 multiwell plate
Life Technologies	D3571	
ThermoFisher Scientific	150350	100 mm diameter dish for tissue culture
Gibco (Life Technologies)	10569-010	Tissue culture medium (500 mL)
VWR	360294H	Mounting medium
Merck	6522	Mounting medium
Sigma-Aldrich	3609	Reagent for TE buffer
CellPath	RBC-0100-00A	Staining reagent
Gibco	10500-064	For use in tissue culture medium
Fisher (Acros)	119690010	10% Formalin
iGenix	IG2095	Microwave used for antigen retrieval
Genta Medical	199050	99% Industrial Denatured Alcohol (IDA)
Akoya Biosciences	InForm	
Leica Biosystems		Automated Vacuum Tissue Processor
Leica Biosystems		Embedding wax bath
Leica Biosystems		Rotary microtome
Leica Biosystems		H&E stainer
Sigma	GHS132-1L	Staining reagent
Merck Milipore	PICMORG50	Organotypic culture insert disc
Leica Biosystems	RE7150-K	DAB staining kit
Akoya Biosciences	FP1500001KT	Fluorophore with Dimethyl Sulfoxide (DMSO) diluent
Akoya Biosciences	FP1487001KT	Fluorophore with Dimethyl Sulfoxide (DMSO) diluent
Akoya Biosciences	FP1488001KT	Fluorophore with Dimethyl Sulfoxide (DMSO) diluent
Akoya Biosciences	FP1495001KT	Fluorophore with Dimethyl Sulfoxide (DMSO) diluent
Akoya Biosciences	FP1496001KT	Fluorophore with Dimethyl Sulfoxide (DMSO) diluent
Akoya Biosciences	FP1497001KT	Fluorophore with Dimethyl Sulfoxide (DMSO) diluent
Akoya Biosciences	FP1501001KT	Fluorophore with Dimethyl Sulfoxide (DMSO) diluent and TSA-DIG reagent

Perkin Elmer	ARH1001EA	HRP polymer
Fisher Scientific	11548876	For use in tissue culture medium
Akoya Biosciences	PhenoChart	Viewer software for scanned images
Thermo Scientific Oxoid	BR0014G	PBS
Perkin Elmer	FP1498	Fluorophore diluent
Invitrogen	P36961	Mounting medium
Perkin Elmer		To load slides into Slide Carrier Hotel for scanning with Vectra Polaris
Fisher Scientific	S/3160/63	10% Formalin
Fisher Scientific	S/4920/53	Reagent for citrate buffer
KEMDENT	1-601	Dental wax surface
Fisher Scientific	10098889	Holder for slides and slide clips
Fisher Scientific	11927774	Slide clips
Sigma-Aldrich	252859	Reagent for TE buffer
Vecta Laboratories	H-1000-10	Mounting medium
Perkin Elmer	Vectra Polaris	Slide scanner
Genta Medical	XYL050	De-waxing agent

14th January 2021



Leicester Cancer Research Centre

Dr Giuditta Viticchié
Leicester Cancer Research Centre
Clinical Sciences Building
Leicester LE2 7LX, UK
Tel: +44 (0)116 223 1857
Email: gv51@le.ac.uk

To: JoVE Methods Collection

Dear Sir/Madam

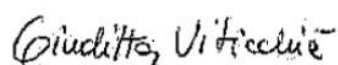
Re: Manuscript number JoVE62130 entitled “Patient-derived tumour explants as a “live” preclinical platform for predicting drug resistance in patients” by Viticchié et al.

Thank you very much for consideration of our manuscript and we are pleased that the editor and reviewers are happy with the manuscript, provided that we address various comments raised by them. We here provide a revised manuscript as well as a rebuttal letter in which we highlight a point-by-point response to the editorial and reviewer comments.

We look forward to hearing from you about this revised manuscript.

Yours,

Giuditta Viticchié



Rebuttal to editorial and reviewer comments

Manuscript by Viticchié et al (JoVE62130) entitled "Patient-derived tumour explants as a "live" preclinical platform for predicting drug resistance in patients"

We thank the editor and reviewers for the comments and are very pleased to see they are all happy with the manuscript provided their various comments can be addressed. Below, we provide a point-by-point response to the comments.

1) *Editorial comments:*

- Please take this opportunity to thoroughly proofread the manuscript to ensure that there are no spelling or grammar issues.

Response: We have attempted to address all spelling and grammar issues in the revised version.

- Please revise the following lines to avoid previously published work: 27-29, 200-201, 209-211, 438-440, 449-461, 525-526.

Response: all revisions have been made

- Please revise the text to avoid the use of any personal pronouns (e.g., "we", "you", "our" etc.).

Response: this has been corrected throughout where possible.

- Please ensure that corresponding reference numbers appear as numbered superscripts before the punctuation.

Response: this has been corrected throughout

- Please use abbreviated forms for durations of less than one day when the unit is preceded by a numeral. Do not abbreviate day, week, month, and year. Examples: 5 h, 10 min, 100 s, 8 days, 10 weeks

Response: this has been corrected throughout

- Please add more details to your protocol steps. Please ensure you answer the "how" question, i.e., how is the step performed? Alternatively, add references to published material specifying how to perform the protocol action.

Response: a better explanation of the assembly of the tissue sections on mIF coverplates has been added to the protocol.

- Line 111: Please specify the details of the human specimens collected (i.e., what specimens, how is the specimen collected, what is the volume of the culture medium)

Response: this information has been provided

- Line 121: Please mention the specifications of the dish used.

Response: Specifications of the material used has been included in the Tables of Materials and a reference within the protocol has been introduced to facilitate the reading.

- Line 123: Please include the details of dental wax surface.

Response: Specifications of the material used has been included in the Tables of Materials and a reference within the protocol has been introduced to facilitate the reading.

- Line 130: Please mention the volume of the culture media used.

Response: this information has now been provided

- Line 137: Please provide the details of the organotypic culture insert.

Response: Specifications of the material used has been included in the Tables of Materials and a reference within the protocol has been introduced to facilitate the reading.

- Line 188-227: What conditions are used for incubation? What are the experimental parameters for the H&E staining?

Response: this information has now been provided

- Line 268: Please specify the volume of UP water used.

Response: this information has now been provided

- Line 277: Please include the details of primary antibody dilution.

Response: Primary antibody dilutions have not been included since we describe a general mIF method that can be applied to a variety of experiments. Experimental dilutions might change according to the antibody brand, specifications and manufacturer guidelines and strictly depend on the choice of the user. It is recommended to test antibody dilutions independently before performing the described technique.

- Line 280: Please specify the volume of PBS used to wash slides.

Response: this information has now been provided

- Please define the abbreviations before use (HRP, DAPI).

Response: this information has now been provided

- JoVE cannot publish manuscripts containing commercial language. This includes trademark symbols (™), registered symbols (®), and company names before an instrument or reagent. Please remove all commercial language from your manuscript and use generic terms instead. All commercial products should be sufficiently referenced in the Table of Materials.

Response: All commercial content has been omitted in the manuscript. Since the protocol was formulated specifically using the software provided by AKOYA Biosciences, references to the user manuals have been added in the Tables of Materials.

- JoVE policy states that the video narrative is objective and not biased towards a particular product featured in the video. The goal of this policy is to focus on the science rather than to present a technique as an advertisement for a specific item. To this end, we ask that you please reduce the number of instances of "Vectra Polaris multispectral automated imaging system" and "InForm" within your text. The term may be introduced but please use it infrequently and when directly relevant. Otherwise, please refer to the term using generic language.

Response: reference to these particular products has been reduced throughout

- Lines 566-570/ 573-581: Please revise the lines in the figure legends to avoid previously published work. The legends can be used if reprint permissions are obtained from the source.

Response: these lines have been revised accordingly

- Please do not use the &-sign or the word "and" when listing authors. Do not use any abbreviations for the journal titles and book titles. Article titles should start with a capital letter and end with a period and should appear exactly as they were published in the original work, without any abbreviations or truncations.

Response: the citation format has been modified as requested.

- Figure 1: Please remove the commercialization content (Vectra Polaris slide scanner and InForm by AKOYA Bio) from the schematic.

Response: the figure has been amended accordingly

- Figure 2: Please include the details of magnification used in the images represented.

Response: the required information has been added to the figure legend.

- Figure 4: Please specify the units on the X and Y-axis. Please include a scale bar for the microscope images as well.

Response: the figure has been amended accordingly

- Please remove trademark (™) and registered (®) symbols from the Table of Equipment and Materials.

Response: this has been amended accordingly

2) Reviewer #1:

Manuscript Summary:

In the manuscript "Patient-derived tumour explants as a "live" preclinical platform for predicting drug resistance in patients" the authors describe their technique for generating PDEs using floating organotypic insert discs, as well as subsequent drug treatment, tissue processing, immunostaining, and multiplex immunofluorescence (mIF). This is a well written protocol that is easy to follow and will be helpful to scientists interested in PDEs.

Major Concerns: None

Minor Concerns:

Grammatical errors

Response: these have been addressed throughout

3) Reviewer #2:

Manuscript Summary:

Very through and detailed methods included

Major Concerns: none

Minor Concerns: Missing reference in the introduction line 70-72. Cancer Lett. 2018 May 1;421:51-58. doi: 10.1016/j.canlet.2018.02.006. Epub 2018 Feb 6.PMID: 29425684. This reference can also be added to discussion

Response: the missing reference has been added to the introduction and discussion.

Section 6.5 Line 257 Add details of the microwave used for antigen retrieval. This is critical for successful antigen retrieval.

Response: Details of the microwave used for antigen retrieval have now been added to the Table of Materials.